Parkinson´s related protein DJ-1 is involved in aberrant cell cycle re-entry through Cdk5

Mª José López-Grueso
Universidad de Cordoba Facultad de Ciencias
Carmen Alicia Padilla
Universidad de Cordoba Facultad de Ciencias
José Antonio Bárcena
Universidad de Cordoba Facultad de Ciencias
Raquel Requejo-Aguilar (bb2reagr@uco.es)
University of Cordoba https://orcid.org/0000-0002-0532-7630

Research

Keywords: DJ-1, Tau, cell cycle, neuronal death, Parkinson disease

Posted Date: February 7th, 2020

DOI: https://doi.org/10.21203/rs.2.22860/v1

Abstract

DJ-1 is a multifunctional protein involved in Parkinson disease (PD) that can act as antioxidant, molecular chaperone, protease, glyoxalase and transcriptional regulator. However, the exact mechanism by which DJ-1 dysfunction contributes to development of Parkinson´s disease remains elusive. Here, using a comparative proteomic analysis between normal cortical neurons and neurons lacking DJ-1, we show that this protein is involved in cell cycle checkpoints disruption as a consequence of increased amount of p-Tau and a-synuclein proteins, altered signalling pathways, as the phosphoinositide-3-kinase/protein kinase B (PI3K/AKT) and mitogen-activated protein kinase (MAPK), and deregulation of cyclin-dependent kinase 5 (Cdk5). Cdk5 is normally involved in dendritic growth, axon formation and the establishment of synapses, but can also contribute to cell cycle progression, as in our case, in pathological conditions. In addition, we observed a decrease in proteasomal activity, probably due to Tau phosphorylation that can also lead to activation of mitogenic signalling pathways. Taken together, our findings indicate, for the first time, that aborted cell cycle re-entry could be at the onset of DJ-1 associated PD. Thereby, new approaches targeting cell cycle re-entry can be envisaged to improve current therapeutic strategies.

Introduction

DJ-1 protein was first described as the product of an oncogene and its high expression was reported in many cancers (1). However, DJ-1 has also been linked to a familiar form of Parkinson´s disease (PD) as well as other neurodegenerative diseases such as Alzheimer disease, Huntington disease and amyotrophic lateral sclerosis (2, 3). The extensive amount of disorders in which DJ-1 is involved, probably due to its multiple functions, makes it difficult to know its exact mechanism of action. However, increased levels of oxidative stress associated with DJ-1 deficiency seem to play a central role in neurodegeneration (3). Emerging evidences indicate that aberrant cell cycle associated to oxidative stress in mature neurons may be behind neurodegeneration. Expression of cell cycle markers in differentiated neurons is necessary to carry out synaptic function, neuronal migration and maturation (4). However, overexpression of these markers can also lead to a cell cycle re-entry, lethal to neurons, through different pathways. Thereby, reactive oxygen species (ROS) mediate oxidative stress-induced DNA damage, ubiquitin proteasome system (UPS) dysfunction, accumulation of toxic proteins such as α-synuclein, parkin, Tau and amyloid β, and activation of signalling pathways including PI3K/Akt, P^{38}/MAPK, Wnt/β-catenin and Notch (5), and subsequent activation of cell cycle. Interestingly DJ-1 has been associated to many of these events. Thus, loss of function or mutation of DJ-1 leads to α-synuclein accumulation and aggregation along with an increase in Tau hyperphosphorylation (6, 7). DJ-1 also participates in the regulation of signalling pathways including MAPK and Akt (8). Finally, DJ-1 has been described to regulate proteasomal activity depending on its oxidation state (9). For this, it would not be surprising that lack of DJ-1 could be related to an abnormal activation of the cell cycle, although this has not been described previously. In this regard, fibroblasts lacking DJ-1 show increased proliferation (10), and

neurons and neural precursors from Pink1 deficient mice, a protein transcriptionally regulated by DJ-1, showed an increase in the number of cells re-entering the cell cycle (11).

Here we combined biochemical and proteomic approaches to study the effect of DJ-1 absence in primary cortical neuron cultures. Our results revealed that lack of DJ-1 up-regulates proteins related to cell cycle control and proliferation, protein translation, proteasome-mediated protein degradation and phagosome maturation. These changes suggest, in a novel way, that lack of DJ-1 leads to cell cycle activation in mature neurons that could be responsible for their death and therefore contribute to the development of Parkinson's disease.

Results

Differential proteomic profiles between wild type and mutant DJ-1 neurons

A comparative proteomic study was carried out to determine the effect of DJ-1 absence on the proteome of cortical neurons. After data filtering and analysis, a total of 2355 proteins were identified (Table S1) of which 139 showed significant variation (Table S2), most of them (~ 80%) being up-regulated in neurons knockout for DJ-1 (Fig. 1A-B). As proof of analysis reliability, the spots corresponding to DJ-1, absent in knockout neurons, and α-synuclein, known to accumulate in the absence of DJ-1 (6, 12), are shown (Fig. 1A). The main decreases were detected in proteins involved in proteolysis; induction of apoptosis; signalling related to cell proliferation and survival such as p21-activated kinase (PAK), phosphatase and tensin homolog (PTEN) and nuclear factor-κB (NF-κB); mitochondrial dysfunction and Parkinson´s disease (Fig. 1B, Supplementary Fig. 1A). The main increases were detected in proteins involved in mRNA splicing, proteasome activity, regulation of translation, Akt and AMPK signalling, and cell cycle control through Cdk5 (Fig. 1C, Supplementary Fig. 1B). The increase in some of these proteins can lead to induction or inhibition of several pathways (Fig. 1D).

Altogether, the changes observed suggest an abnormal entry into the cell cycle that can be responsible for neuronal death associated to PD onset.

α-synuclein and p-Tau accumulation is associated to DJ-1 deficiency in primary neuron cultures

Accumulation of unfolded protein forming aggregates is a hallmark of most neurodegenerative diseases including PD. For that, it is not surprising that DJ-1 deficiency has been associated with aggregation not only of α-synuclein but also of other proteins such as p-Tau (6, 7). Our results show that DJ-1 deficient primary neurons have increased amounts of both α-synuclein and p-Tau and no significant increase in the amount of unphosphorylated Tau and β-amyloid (Fig. 2A-D) (Supplementary Fig. 2).

These data indicate that DJ-1 might play a role in α-synuclein aggregation and Tau phosphorylation.

Tau hyperphosphorylation in DJ-1 knockout neurons seems to be mediated by Cdk5 and directly by Akt and AMPK

Proteins related to Cdk5 signalling were upregulated in dj1$^{-/-}$ neurons (Fig. 1D) in parallel with an increase in Tau phosphorylation. Cdk5 has been described to directly phosphorylate Tau and other proteins such as MAP2 and MAP1b (13), and we have also observed an increased phosphorylation in these two proteins (Fig. 3A) (Supplementary Fig. 2). Another mechanism to increase p-Tau seems to be related directly to Akt, since canonical Akt pathway is inhibited in dj1$^{-/-}$ neurons (Fig. 1D) and inhibition of mTOR pathway was also observed (Fig. 3B-D and Fig. 1D). Some authors have described an increase of Tau phosphorylation through Akt/GSK-3β pathway in neuroblastoma cells when DJ-1 was mutated (7). However, we did not observe changes in Akt/GSK-3β pathway since GSK-3β levels were similar in both dj1$^{+/+}$ and dj1$^{-/-}$ neurons (Fig. 3E) and no phosphorylation of this protein was detected. Nonetheless, GSK-3α levels were significantly increased in the mutant (Fig. 3E) suggesting that this isoform might play a role in Tau phosphorylation since it shares many substrates and functions with GSK-3β (14). In fact, both GSK3α and β have been widely related with Alzheimer pathogenesis (15) and both interact with Tau (16). On the other hand, an increase in Akt phosphorylation level was observed in DJ-1 knockout neurons (Fig. 3G). Akt has been described to phosphorylate Tau in vitro (17), thus, it would not be surprising if the same happens in vivo. Finally, AMPK signalling pathway, that is activated in dj1$^{-/-}$ neurons (Supplementary Fig. 1B), has been also involved in Tau hyperphosphorylation (18).

Factors that trigger cell cycle re-entry are increased in DJ-1 deficient neurons

Accumulation of α-synuclein and p-Tau, and changes in Akt pathway, described above for dj1$^{-/-}$ neurons, have also been described to force cell cycle re-entry in mature neurons leading to cell death as reported for PD and other neurodegenerative diseases (5). In this regard, the role of Cdk5 should be highlighted because we observed an increase in Cdk5 signalling (Fig. 1D) and changes in cell cycle checkpoints in neurons deficient for DJ-1 (Supplementary Fig. 1B). Cdk5 is not only involved in Tau hyperphosphorylation, but also, in apoptotic neuronal death and cell cycle regulation. In mature neurons, Cdk5 is involved in axonal guidance and synaptic function, but in pathological conditions, such as accumulation of amyloid-β and prion peptides, it is able to induce proteins involved in reactivating cell cycle from G0 in mature neurons (19). Phospho-retinoblastoma and proliferating cell nuclear antigen (PCNA) is among the cell cycle related proteins induced by Cdk5 (19). Here, we show that dj-1$^{-/-}$ neurons have increased levels of PCNA (Fig. 4A) suggesting, as in previous reports, that neurons pass the S phase and die when they reach G2/M checkpoint. In addition, the proteomic analysis revealed the increase in other proteins in neurons lacking DJ-1 as shown for MAPK3 (ERK1) (Fig. 4B), which can support a transition from G1 to S phase. Moreover, a decrease in brain derived neurotrophic factor (BDNF) receptor expression was observed in dj1 $^{-/-}$ neurons (Fig. 4C). BDNF has been described to downregulate cyclin B expression and Cdk1 activity in neurons, contributing to blockade of G2/M transition (20). Thus, the

decrease in BDNF receptor we have observed in dj-$1^{-/-}$neurons could release this blockade and stimulate cell cycle progression from G2 to M phase leading to cell death at this point of post-mitotic neurons.

Another factor contributing to cyclins expression and cell cycle re-entry is the production of advanced glycation end products (AGEs) (21). We analysed protein glycation and found that it was increased in neurons lacking DJ-1 (Fig. 4D). Thereby, AGEs increase in dj$1^{-/-}$ neurons may be another factor contributing to cell cycle activation and neuronal death.

Finally, we detected up-regulation of proteasome related proteins (Fig. 1C). Loss of function of ubiquitin proteasome system (UPS) is involved in the pathogenesis of PD and other neurodegenerative diseases (22). Additionally, Tau phosphorylation leads to malfunction of UPS and cyclins accumulation that induce neurons re-entry into the cell cycle (5). We observed a general up-regulation of proteins that form the proteasome in neurons lacking DJ-1 (Fig. 4E), probably due to a compensatory mechanism, because when proteasome activity was analysed a decrease in the activity was observed (Fig. 4F). Thus, loss of activity of UPS, probably due to the increase in Tau phosphorylation, observed in dj$1^{-/-}$ neurons, may contribute to cell cycle activation by cyclins that normally are degraded and consequently resulting in death of these neurons.

Discussion

Our results point to cell-cycle re-entry as the cause of neuronal death associated to DJ-1 deficiency. Many of the pathways we have observed changing in neurons lacking DJ-1 have been implicated in cell cycle re-entry in neurodegeneration and neuromuscular disorders including Parkinson´s, Alzheimer or Huntington diseases (5). Furthermore, the idea of cell cycle re-entry as the cause of neuronal death associated to DJ-1 deficiency is supported by the fact that lack of DJ-1 produces oxidative stress (3), which is one of the main causes reported for inducing cell cycle abnormalities in post-mitotic neurons (5)

The proteomic analysis reveals that DJ-1 deficiency alters cell cycle checkpoints through Cdk5 signalling up-regulation (Fig. 5). Cdk5 acts in postmitotic neurons controlling functions such as axonal guidance and synapse regulation (19). However, under pathological conditions, as is the case in our experimental model of increased oxidative stress associated to DJ-1 deficiency, Cdk5 induces cell cycle proteins and forces mature neurons to reactivate it (19). The increase in PCNA observed in dj$1^{-/-}$ neurons indicates a progression in the cell cycle at least until G2 phase in these neurons, in agreement with the model proposed for other pathologies (19). This may be mediated by the increase in Tau phosphorylation (13) that contributes to DNA damage and activation of mitogenic signals as well as cyclins and Cdks imbalance by UPS dysfunction (5).

In fact, DJ-1 mutations have been related to Tau hyperphosphorylation (7) and it has been widely described that DJ-1 colocalises with Tau inclusions in brains from PD patients indicating that DJ-1 can act as a chaperone modulating the aggregation and toxicity of Tau as has been demonstrated for other

proteins that form inclusions such as α-synuclein, mutant huntingtin and microtubule associated protein 1B (MAP1B) (23–25).

Here, we show how DJ-1 deficient neurons show increased levels of Tau phosphorylation and decreased proteasome activity that, along with up-regulation of Cdk5 signalling, agree with re-entry into the cell cycle as a possible cause of neuronal death. Neurodegeneration associated to cell cycle re-entry is also related to disturbances in signalling pathways involving proteins such as Notch, Wnt, Akt and MAPK (5). AMPK and p-Akt have been related to Tau phosphorylation (17, 18) and MAPK signalling pathway is activated and initiate cell cycle in post-mitotic hippocampal neurons after a lesion by increased expression of cyclin D (26). Thereby, the up-regulation of AMPK signalling, inhibition of PI3K/Akt/mTOR signalling but with the increase in Akt phosphorylation, and increase in MAPK3 (ERK1) protein, that we observed in neurons lacking DJ-1 can account for an aberrant activation of the cell cycle.

AGEs are increased in neurons lacking DJ-1. AGEs are mostly produced from methylglyoxal, an inevitable by-product of glycolysis (27), and mouse embryonic fibroblasts (MEFs) deficient for protein DJ-1 have been described to increase their glycolytic rate (10). Thus, is not surprising that $dj1^{-/-}$ neurons showed an increase in glycated protein. The observed increase in AGEs in neurons lacking DJ-1 could also contribute to cell cycle activation since it has been shown that AGEs produced as a consequence of oxidative stress, act as mitogenic compounds inducing expression of cyclin D and DNA replication in a mouse model of Alzheimer disease deficient for apolipoprotein E (21).

Finally, other triggering factors contributing to cell cycle activation like UPS dysfunction and deprivation of the brain derived neurotrophic factor (BDNF) and its receptor [5], were also found in $dj1^{-/-}$ neurons, supporting the idea of cell cycle re-entry as the cause of neuronal death. Thus, targeting aberrant cell cycle progression by using cyclins and Cdks inhibitors or molecules that induce cell cycle arrest could be a promising therapeutic strategy for PD treatment.

Methods

Ethical statement regarding the use of animals. Mice were bred at the Animal Experimentation Unit of the University of Córdoba, and all protocols were approved by the Bioethics Committee of the University of Córdoba in accordance with the Spanish legislation (RD53/2013). DJ-1 knockout mice were generously donated by Juan Pedro Bolaños (Institute of Functional Biology and Genomics, Salamanca, Spain) (28); back-crossed for at least eleven generations with C57Bl/6J WT mice for the experiments and bred under homozygosis.

Cell cultures. Cortical neurons in primary culture were prepared from foetal (E15.5) $dj1^{-/-}$ (DJ-1 KO) and $dj1^{+/+}$ (WT) offspring. Cells were seeded at 1.8×10^5 cells cm^{-2} in cell culture plastic dishes previously coated with poly-D-lysine (15 μg ml^{-1}) in neurobasal medium containing 2% of B-27 supplement (Gibco

Brl-Life Technologies, Grand Island, NJ, USA) and 2mM L-glutamine. Neurons were incubated at 37 °C in a humidified 5% CO_2-containing atmosphere; at second day, the medium was replaced, and neurons were used on the seventh or eighth day in vitro.

Sample preparation. Cortical neurons grown for 7-8 days were harvested and lysed in 100mM Tris-HCl buffer, pH 7.5, using a homogenization pestle for 1.5 mL tubes. The extracts were centrifuged, and the supernatants stored at −80 °C until use for mass spectrometry or western blot analysis. For the determination of proteasome activity the neuron pellet was homogenized with sea-sand in Tris-HCl buffer (0.5mM EDTA, 1mM PMSF, 100mM Tris-HCl, pH 7.5). The samples were centrifuged, and the supernatant fraction was collected for analysis.

Mass spectrometry.

Sample preparation, digestion and nLC-MS2 analysis. Samples from supernatants were prepared and analyzed in the Proteomics Facility at Research Support Central Service (SCAI), University of Cordoba. Protein extracts were cleaned-up in 10% 1D SDS-PAGE. The gel was stained with Coomassie Blue and protein bands were cut off, diced and kept in water until digestion. Gel dices were firstly distained and protein resuspended and reduced by addition of 20mM dithiothreitol. The mixture was cooled down to room temperature and alkylatated by addition of 40mM iodoacetamide. Proteolytic digestion was performed by addition of Trypsin (Promega, Madison, WI) and stopped by addition of trifluoroacetic acid, the digested samples were finally Speedvac dried. Nano-LC was performed in a Dionex Ultimate 3000 nano UPLC (Thermo Scientific) as described previously (29).

Data analysis. MaxQuant (v1.5.7.0) (30) and Perseus (v1.5.6.0) (31) software were used to analyze the different MSe runs in triplicate. Proteins were identified by searching raw data against the mouse UniprotKB/Swiss-Prot protein database (February 2018 version). Carbamidomethylation of cysteines as fixed modification, and oxidation of methionine and phosphorylation (ST) (Y) as variable modifications, were set for the study. Cleavage specificity was by trypsin, allowing for a maximum of one missed cleavage, a mass tolerance of 10 ppm for precursors and 0.01 Da for fragment ions. The false discovery rate (FDR) cut-off for protein identification was 1%. Enabling the “match between runs” option allowed for identification transfer between samples. Similar proteins were grouped, and only unique peptides were used for quantification. Identified from reverse database or contaminant hit proteins were removed prior to further analysis. Finally, the resultant list was analyzed according to the instructions of the software developers (31). The criteria for considering a differentially expressed protein were that it was identified and quantified using at least two unique peptides and had a $P \leq 0.05$ value. (Supplementary Tables S1 and S2). The same criteria were used to identify peptide phosphorylation including a value of posterior

error probability (PEP)≤0.05 (Supplementary Table S3). Functional enrichment analysis was carried out using Ingenuity Pathways Analysis tool (IPA-Ingenuity Systems, www.ingenuity.com) and the results compared with other tools such as GOrilla, David and String (32-34).

Western blot. Cells were lysed in 50mM Tris-HCl buffer, pH 7.5 supplemented with 2% sodium dodecyl sulphate (SDS), 2mM EDTA, 2mM EGTA, , phosphatase inhibitor (50mM NaF) and protease inhibitors (100 mM phenylmethylsulphonyl fluoride, 50 μg ml^{-1} amastatin and 50 μg ml^{-1} leupeptin), stored on ice for 30 min and boiled for 10 min. Extracts (25–100 μg) were subjected to SDS–PAGE and blotted onto nitrocellulose membrane (GE Healthcare Life Sciences). After electrotransfer, membranes were blocked for 1 h with 5% non-fat milk (BioRad) solubilized in TBS-T (150mM NaCl, 50mM Tris, pH 7.5, 0.05% Tween-20). Primary antibodies were anti-AGEs (1:100; ab23722; Abcam), anti-mTOR Pathway Antibody Sampler Kit (1:1000; Cell Signalling), anti-Akt (1:1000; sc-5298; Santa Cruz Biotechnology), anti-p-Akt (1:1000; 4060S; Cell Signalling), anti-DJ-1 (1:2000; PA1-46262, Invitrogen), and anti-b-actin (1:2000; sc-47778; Santa Cruz Biotechnologies);. Secondary antibodies were anti-rabbit (1:4000) and anti-mouse (1:8000) IgG-peroxidase conjugates (Sigma). Incubations were carried out overnight and for 2 h, respectively. Signal detection was performed with an enhanced chemiluminescence kit (ECL Plus Western blotting detection reagent from GE Healthcare). Western blots were done at least in triplicate and represent independent replicate experiments. The protein abundances were measured by densitometry of the bands on the membranes using ImageJ 1.48u4 software (National Institutes of Health, USA), and normalized against the corresponding b-actin band.

Proteasome activity assay. Cells from three independent experiments were lysed as described above. The proteasomal activity was measured using the 20S Proteasome Activity Assay kit according to the manufacturer's instructions (APT280, Chemicon, Millipore). Proteasome activity is expressed as AMC (7-amino-4-methylcoumarin) relative fluorescent units (RFU) with the signal of the fraction inhibited with Lactacystin, an inhibitor of the 20S proteasome β5subunit provided in the kit, as a reference.

Protein determination. Protein concentrations were determined in the lysates or in parallel cell culture incubations after solubilization with 0.1 M NaOH. Protein concentrations were determined using a Pierce BCA Protein Assay kit (Thermo Scientific, Milan, Italy) with bovine serum albumin as a standard.

Statistical analysis. All measurements in cell culture were carried out, at least, in triplicate, and the results are expressed as the mean ± SEM values from at least three different culture preparations. Two groups

were compared and statistical analysis of the results was performed by one-way analysis of variance (ANOVA), followed by the Student's t test. In all cases, $p<0.05$ was considered significant.

Abbreviations

Parkinson disease (PD)

Phosphoinositide-3-kinase/protein kinase B (PI3K/AKT)

Mitogen-activated protein kinase (MAPK)

Cyclin-dependent kinase 5 (Cdk5)

Reactive oxygen species (ROS)

Ubiquitin proteasome system (UPS)

p21-activated kinase (PAK)

Phosphatase and tensin homolog (PTEN)

Nuclear factor-kB (NF-kB)

Phospho-retinoblastoma and proliferating cell nuclear antigen (PCNA)

Brain derived neurotrophic factor (BDNF)

Advanced glycation end products (AGEs)

Microtubule associated protein 1B (MAP1B)

Proteomics Facility at Research Support Central Service (SCAI)

False discovery rate (FDR)

Ingenuity Pathways Analysis tool (IPA)

Sodium dodecyl sulphate (SDS)

Relative fluorescent units (RFU)

One-way analysis of variance (ANOVA)

Declarations

Ethics approval and consent to participate: Mice were bred at the Animal Experimentation Unit of the University of Córdoba, and all protocols were approved by the Bioethics Committee of the University of Córdoba in accordance with the Spanish legislation (RD53/2013). DJ-1 knockout mice were generously donated by Juan Pedro Bolaños (Institute of Functional Biology and Genomics, Salamanca, Spain); back-crossed for at least eleven generations with C57Bl/6J WT mice for the experiments and bred under homozygosis.

Consent for publication: Not applicable.

Availability of data and materials: Please contact author for data requests.

Funding: Spanish Ministry of Industry and Competitiveness [Grant BFU2016-80006-P], The Andalusian Regional Government [Group BIO-216] and the University of Córdoba [XX PP, Mod. 5.4].

Competing interests: The authors declare that they have no competing interests.

Author contributions: RRA conceived the project. RRA, CAP and JAB designed and coordinated the experiments. MLG and RRA performed the experiments and analysed the data. RRA wrote this manuscript, and CAP and JAB rebirvised this manuscript.

Acknowledgements: We thank Dr. Juan Pedro Bolaños (Instituto de Biología Funcional y Genómica) for generously providing us with mice mutants for DJ-1 protein. This work was supported by the Spanish Ministry of Industry and Competitiveness [Grant BFU2016-80006-P], The Andalusian Regional Government [Group BIO-216] and the University of Córdoba [XX PP, Mod. 5.4]. Technical support from the Proteomics Unit, SCAI, University of Córdoba and assistance provided by the PAB (Andalusian Bioinformatics Platform) centre located at the University of Málaga (www.scbi.uma.es) are acknowledged.

References

1. Nagakubo D, Taira T, Kitaura H, Ikeda M, Tamai K, Iguchi-Ariga SM, et al. DJ-1, a novel oncogene which transforms mouse NIH3T3 cells in cooperation with ras. Biochem Biophys Res Commun. 1997;231(2):509-13.
2. Bonifati V, Rizzu P, van Baren MJ, Schaap O, Breedveld GJ, Krieger E, et al. Mutations in the DJ-1 gene associated with autosomal recessive early-onset parkinsonism. Science. 2003;299(5604):256-9.
3. Ariga H. DJ-1/Park7 protein. New York, NY: Springer Berlin Heidelberg; 2017. pages cm p.
4. Lim S, Kaldis P. Cdks, cyclins and CKIs: roles beyond cell cycle regulation. Development. 2013;140(15):3079-93.
5. Sharma R, Kumar D, Jha NK, Jha SK, Ambasta RK, Kumar P. Re-expression of cell cycle markers in aged neurons and muscles: Whether cells should divide or die? Biochim Biophys Acta Mol Basis Dis. 2017;1863(1):324-36.
6. Xu CY, Kang WY, Chen YM, Jiang TF, Zhang J, Zhang LN, et al. DJ-1 Inhibits alpha-Synuclein Aggregation by Regulating Chaperone-Mediated Autophagy. Front Aging Neurosci. 2017;9:308.
7. Wang Y, Liu W, He X, Zhou F. Parkinson's disease-associated DJ-1 mutations increase abnormal phosphorylation of tau protein through Akt/GSK-3beta pathways. J Mol Neurosci. 2013;51(3):911-8.
8. Oh SE, Mouradian MM. Regulation of Signal Transduction by DJ-1. Adv Exp Med Biol. 2017;1037:97-131.
9. Moscovitz O, Ben-Nissan G, Fainer I, Pollack D, Mizrachi L, Sharon M. The Parkinson's-associated protein DJ-1 regulates the 20S proteasome. Nat Commun. 2015;6:6609.
10. Requejo-Aguilar R, Lopez-Fabuel I, Jimenez-Blasco D, Fernandez E, Almeida A, Bolanos JP. DJ1 represses glycolysis and cell proliferation by transcriptionally up-regulating Pink1. Biochem J. 2015;467(2):303-10.
11. Requejo-Aguilar R, Lopez-Fabuel I, Fernandez E, Martins LM, Almeida A, Bolanos JP. PINK1 deficiency sustains cell proliferation by reprogramming glucose metabolism through HIF1. Nat Commun. 2014;5:4514.
12. Nash Y, Schmukler E, Trudler D, Pinkas-Kramarski R, Frenkel D. DJ-1 deficiency impairs autophagy and reduces alpha-synuclein phagocytosis by microglia. J Neurochem. 2017;143(5):584-94.
13. Castro-Alvarez JF, Uribe-Arias SA, Mejia-Raigosa D, Cardona-Gomez GP. Cyclin-dependent kinase 5, a node protein in diminished tauopathy: a systems biology approach. Front Aging Neurosci. 2014;6:232.
14. Beurel E, Grieco SF, Jope RS. Glycogen synthase kinase-3 (GSK3): regulation, actions, and diseases. Pharmacol Ther. 2015;148:114-31.
15. Ma T. GSK3 in Alzheimer's disease: mind the isoforms. J Alzheimers Dis. 2014;39(4):707-10.
16. Sun W, Qureshi HY, Cafferty PW, Sobue K, Agarwal-Mawal A, Neufield KD, et al. Glycogen synthase kinase-3beta is complexed with tau protein in brain microtubules. J Biol Chem. 2002;277(14):11933-40.

17. Ksiezak-Reding H, Pyo HK, Feinstein B, Pasinetti GM. Akt/PKB kinase phosphorylates separately Thr212 and Ser214 of tau protein in vitro. Biochim Biophys Acta. 2003;1639(3):159-68.
18. Domise M, Vingtdeux V. AMPK in Neurodegenerative Diseases. Exp Suppl. 2016;107:153-77.
19. Lopes JP, Oliveira CR, Agostinho P. Cdk5 acts as a mediator of neuronal cell cycle re-entry triggered by amyloid-beta and prion peptides. Cell Cycle. 2009;8(1):97-104.
20. Ovejero-Benito MC, Frade JM. Brain-derived neurotrophic factor-dependent cdk1 inhibition prevents G2/M progression in differentiating tetraploid neurons. PLoS One. 2013;8(5):e64890.
21. Kuhla A, Ludwig SC, Kuhla B, Munch G, Vollmar B. Advanced glycation end products are mitogenic signals and trigger cell cycle reentry of neurons in Alzheimer's disease brain. Neurobiol Aging. 2015;36(2):753-61.
22. Zheng Q, Huang T, Zhang L, Zhou Y, Luo H, Xu H, et al. Dysregulation of Ubiquitin-Proteasome System in Neurodegenerative Diseases. Front Aging Neurosci. 2016;8:303.
23. Zondler L, Miller-Fleming L, Repici M, Goncalves S, Tenreiro S, Rosado-Ramos R, et al. DJ-1 interactions with alpha-synuclein attenuate aggregation and cellular toxicity in models of Parkinson's disease. Cell Death Dis. 2014;5:e1350.
24. Wang Z, Zhang Y, Zhang S, Guo Q, Tan Y, Wang X, et al. DJ-1 can inhibit microtubule associated protein 1 B formed aggregates. Mol Neurodegener. 2011;6:38.
25. Repici M, Giorgini F. DJ-1 in Parkinson's Disease: Clinical Insights and Therapeutic Perspectives. J Clin Med. 2019;8(9).
26. Hernandez-Ortega K, Arias C. ERK activation and expression of neuronal cell cycle markers in the hippocampus after entorhinal cortex lesion. J Neurosci Res. 2012;90(11):2116-26.
27. Allaman I, Belanger M, Magistretti PJ. Methylglyoxal, the dark side of glycolysis. Front Neurosci. 2015;9:23.
28. Flicek P, Amode MR, Barrell D, Beal K, Brent S, Chen Y, et al. Ensembl 2011. Nucleic Acids Res. 2011;39(Database issue):D800-6.
29. Padilla CA, Barcena JA, Lopez-Grueso MJ, Requejo-Aguilar R. The regulation of TORC1 pathway by the yeast chaperones Hsp31 is mediated by SFP1 and affects proteasomal activity. Biochim Biophys Acta Gen Subj. 2019;1863(3):534-46.
30. Cox J, Mann M. MaxQuant enables high peptide identification rates, individualized p.p.b.-range mass accuracies and proteome-wide protein quantification. Nat Biotechnol. 2008;26(12):1367-72.
31. Tyanova S, Temu T, Cox J. The MaxQuant computational platform for mass spectrometry-based shotgun proteomics. Nat Protoc. 2016;11(12):2301-19.
32. Eden E, Navon R, Steinfeld I, Lipson D, Yakhini Z. GOrilla: a tool for discovery and visualization of enriched GO terms in ranked gene lists. BMC Bioinformatics. 2009;10:48.
33. Huang DW, Sherman BT, Tan Q, Kir J, Liu D, Bryant D, et al. DAVID Bioinformatics Resources: expanded annotation database and novel algorithms to better extract biology from large gene lists. Nucleic Acids Res. 2007;35(Web Server issue):W169-75.

34. Szklarczyk D, Franceschini A, Wyder S, Forslund K, Heller D, Huerta-Cepas J, et al. STRING v10: protein-protein interaction networks, integrated over the tree of life. Nucleic Acids Res. 2015;43(Database issue):D447-52.

Figures

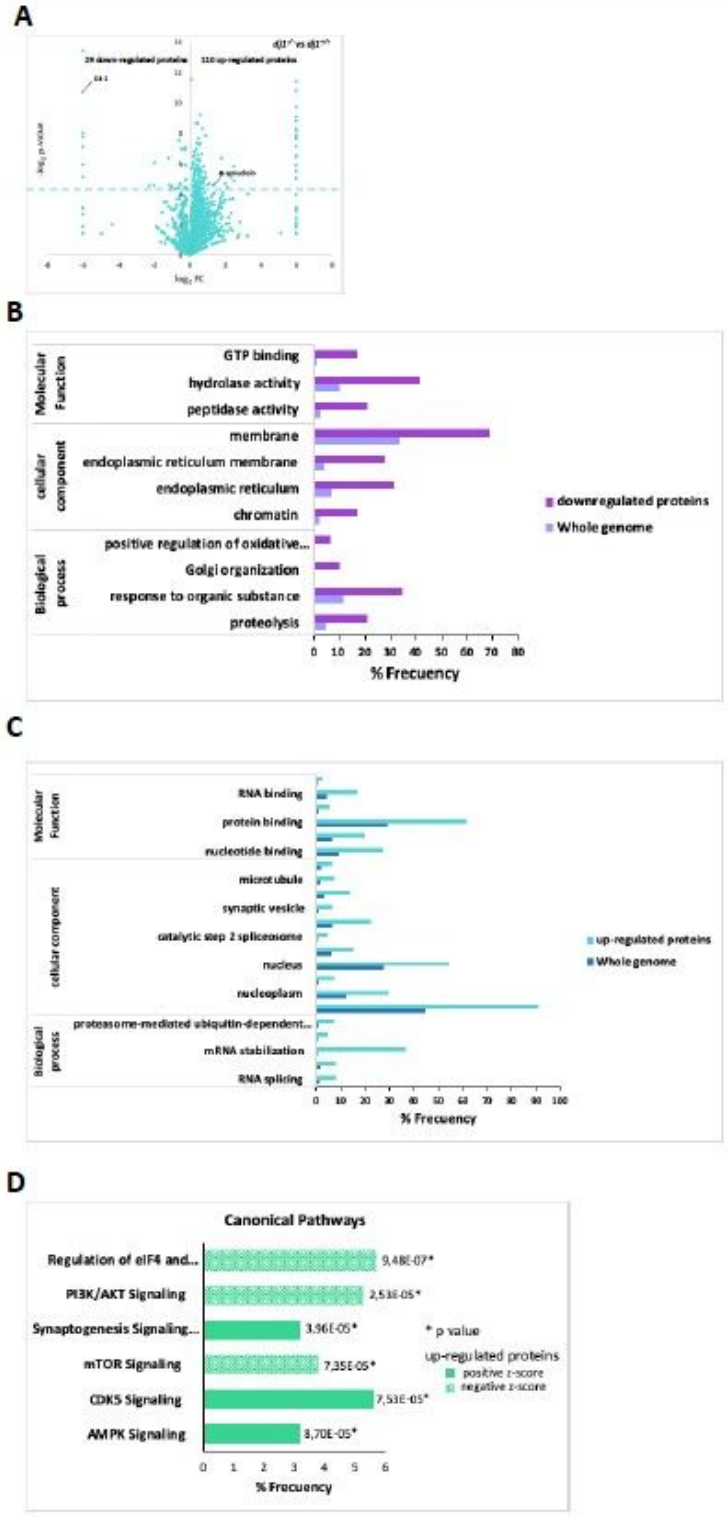

Figure 1

Label-free quantitative (LFQ) Proteomic analysis of changes in DJ-1 knockout (dj1-/–KO) primary cultured neurons. (A) Volcano plot showing the outcome of neurons dj1-/- vs dj1+/+, t-test performed with Perseus. Proteins are distributed along x axis by fold change and y axis by p-value; proteins over the dashed line represent those changing significantly in the absence of DJ-1. (B-D) Gene ontology and Ingenuity pathways enrichment analysis. Enrichment analysis was performed by GO terms using GOrilla,

String and David tools and also Ingenuity Pathways Analysis tool (IPA). Panels B and C show GO biological terms, cellular components and molecular functions clusters that are down or up-regulated in neurons lacking DJ-1 protein, respectively. Panel D shows canonical pathways more significantly altered in DJ-1 deficient neurons detected by IPA indicating induction or inhibition for the different pathways identified.

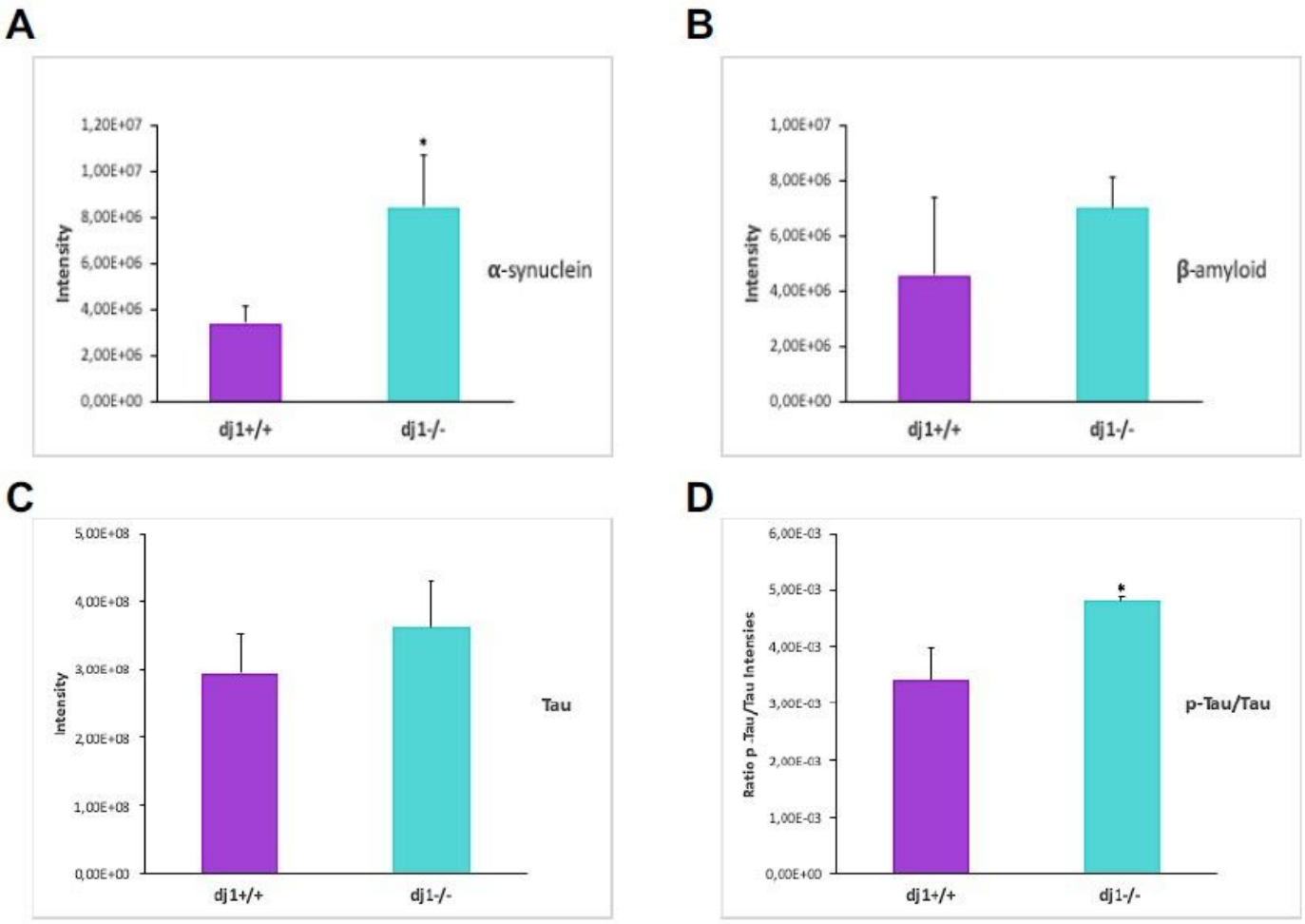

Figure 2

Quantitation of a-synuclein, b-amyloid and Tau in dj1-/- neurons. Levels of a-synuclein (A), b-amyloid (B) and Tau (C) were detected by mass spectrometry and statistically analysed using Perseus. Phosphorylated Tau peptides were also analysed using MaxQuant and the ratio p-Tau/Tau was calculated (D). * indicates significant differences with $p<0.05$.

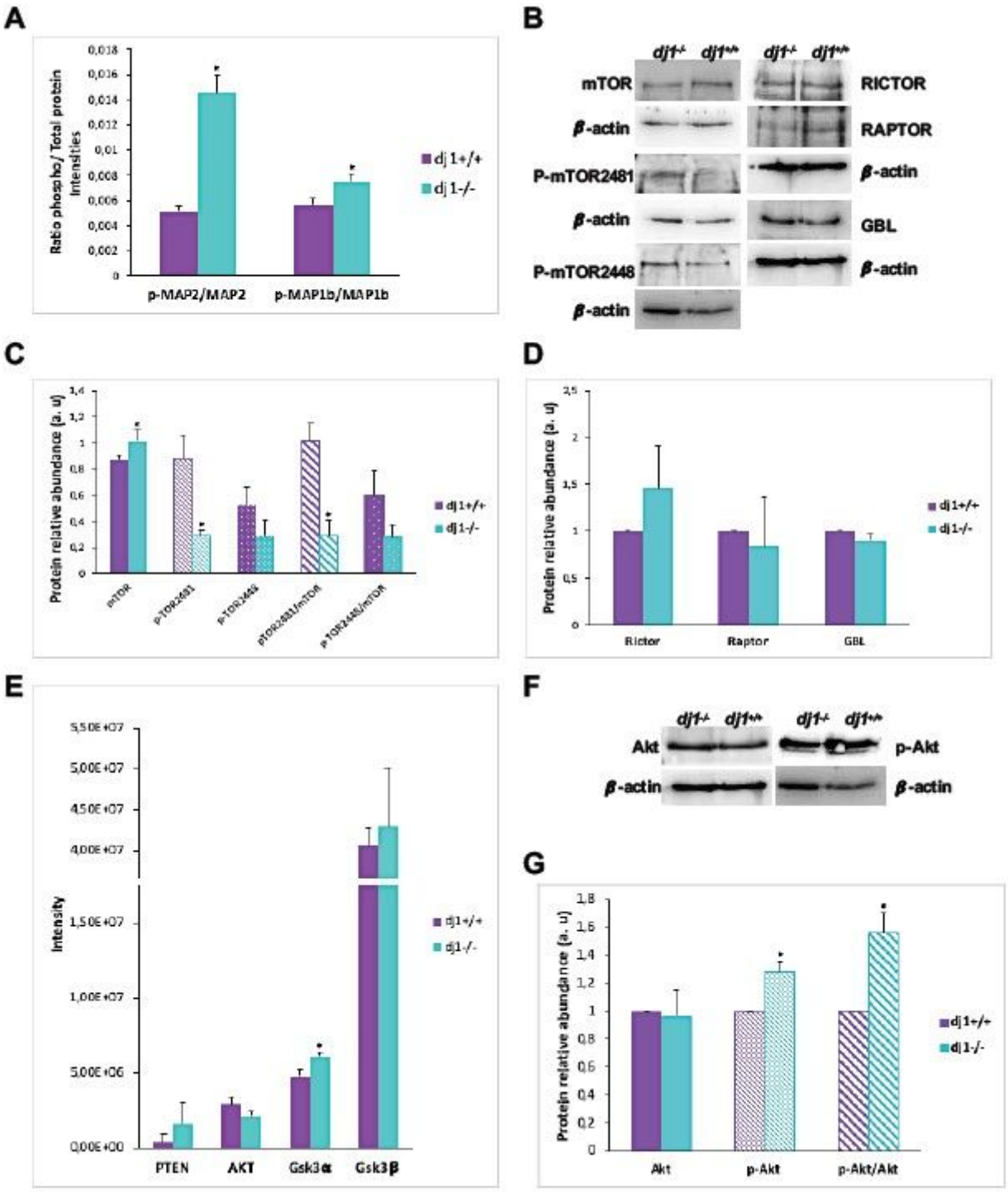

Figure 3

Analysis of proteins related to Cdk5, Akt/GSK and mTOR pathways involved in cell cycle re-entry in mature neurons when DJ-1 is absent. (A) Ratio phospho/ total protein levels for the two targets of Cdk5 MAP2 and MAP1b as quantitated from the MS/MS spectra. (B-D) Western blot analysis and quantification of proteins belonging to mTOR pathway, including the two phosphorylated forms of mTOR, p-mTOR2481 (auto-phosphorylated residue) and p-mTOR2448 (phosphorylated by Akt), in control and

neurons deficient for DJ-1 protein (a representative gel and global densitometry analysis are shown). (E) Levels of proteins related to Akt/GSK pathway identified by mass spectrometry. (F-G) Western blot analysis and quantification of Akt and phospho-Akt in neuron wild type and knockouts for DJ-1 protein. Western blot data are mean ± SD (N≥3; t-test; *p<0.05).

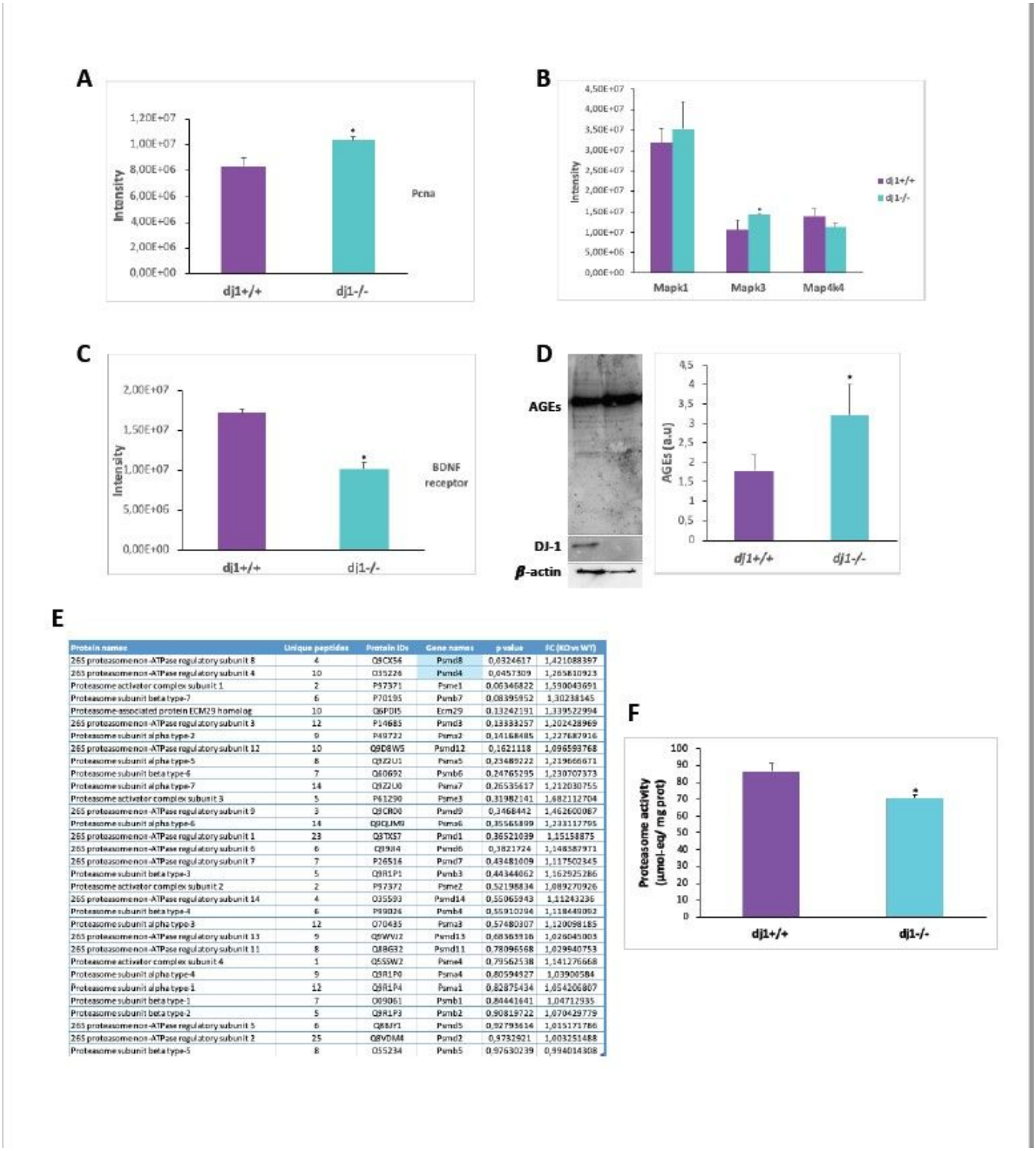

Protein names	Unique peptides	Protein IDs	Gene names	p value	FC (KOvs WT)
26S proteasome non-ATPase regulatory subunit 8	4	Q8CX56	Psmd8	0,0324617	1,421088397
26S proteasome non-ATPase regulatory subunit 4	10	O35226	Psmd4	0,0457309	1,265810923
Proteasome activator complex subunit 1	2	P97371	Psme1	0,06346822	1,590043691
Proteasome subunit beta type-7	6	P70195	Psmb7	0,08395952	1,30238145
Proteasome-associated protein ECM29 homolog	10	Q8PDI5	Ecm29	0,13242191	1,339522994
26S proteasome non-ATPase regulatory subunit 3	12	P14685	Psmd3	0,13333257	1,202428969
Proteasome subunit alpha type-2	9	P49722	Psma2	0,14168485	1,227687916
26S proteasome non-ATPase regulatory subunit 12	10	Q9D8W5	Psmd12	0,1621118	1,096593768
Proteasome subunit alpha type-5	8	Q3Z2U1	Psma5	0,23489222	1,219666871
Proteasome subunit beta type-6	7	Q60692	Psmb6	0,24765295	1,230707373
Proteasome subunit alpha type-7	14	Q9Z2U0	Psma7	0,26535617	1,212030755
Proteasome activator complex subunit 3	5	P61290	Psme3	0,31982141	1,682112704
26S proteasome non-ATPase regulatory subunit 9	3	Q3CRD0	Psmd9	0,3468442	1,462600087
Proteasome subunit alpha type-6	14	Q9QUM9	Psma6	0,35565899	1,233117795
26S proteasome non-ATPase regulatory subunit 1	23	Q3TXS7	Psmd1	0,36521039	1,15158875
26S proteasome non-ATPase regulatory subunit 6	6	Q9JI14	Psmd6	0,3821724	1,148587971
26S proteasome non-ATPase regulatory subunit 7	7	P26516	Psmd7	0,43481009	1,117502345
Proteasome subunit beta type-3	5	Q9R1P1	Psmb3	0,44344062	1,162925286
Proteasome activator complex subunit 2	2	P97372	Psme2	0,52198834	1,089270926
26S proteasome non-ATPase regulatory subunit 14	4	O35593	Psmd14	0,55065943	1,11243236
Proteasome subunit beta type-4	6	P99026	Psmb4	0,55910294	1,118449093
Proteasome subunit alpha type-3	12	O70435	Psma3	0,57480307	1,120098185
26S proteasome non-ATPase regulatory subunit 13	9	Q9WVJ2	Psmd13	0,68363916	1,026045003
26S proteasome non-ATPase regulatory subunit 11	8	Q8BG32	Psmd11	0,78096568	1,029940753
Proteasome activator complex subunit 4	1	Q5SSW2	Psme4	0,79562538	1,141276668
Proteasome subunit alpha type-4	9	Q9R1P0	Psma4	0,80594927	1,03900584
Proteasome subunit alpha type-1	12	Q8R1P4	Psma1	0,82875434	1,054206807
Proteasome subunit beta type-1	7	O09061	Psmb1	0,84441641	1,04712935
Proteasome subunit beta type-2	5	Q9R1P3	Psmb2	0,90819722	1,070429779
26S proteasome non-ATPase regulatory subunit 5	6	Q8BFY1	Psmd5	0,92793614	1,015171786
26S proteasome non-ATPase regulatory subunit 2	25	Q8VDM4	Psmd2	0,9732921	1,003251488
Proteasome subunit beta type-5	8	O55234	Psmb5	0,97630239	0,994014308

Figure 4

Analysis of cell cycle enhancing factors in neurons control and dj1-/-. Levels of the protein PCNA implicated in cell cycle progression (A), MAPKs identified by mass spectrometry (B), and BDNF receptor (C) identified and quantified by mass spectrometry, are shown. (D) Western blot and quantification of advanced ends glycation products (AGEs) (a representative gel and global densitometry analysis are shown). (E) Proteasome proteins identified by mass spectrometry and the fold change dj1-/- vs dj1+/+ are shown, highlighted are proteins with significant changed according to Perseus. (F) Proteasome activity was also determined in these neurons, data are mean ± SD (N≥3, n=3; t-test; *p<0.05).

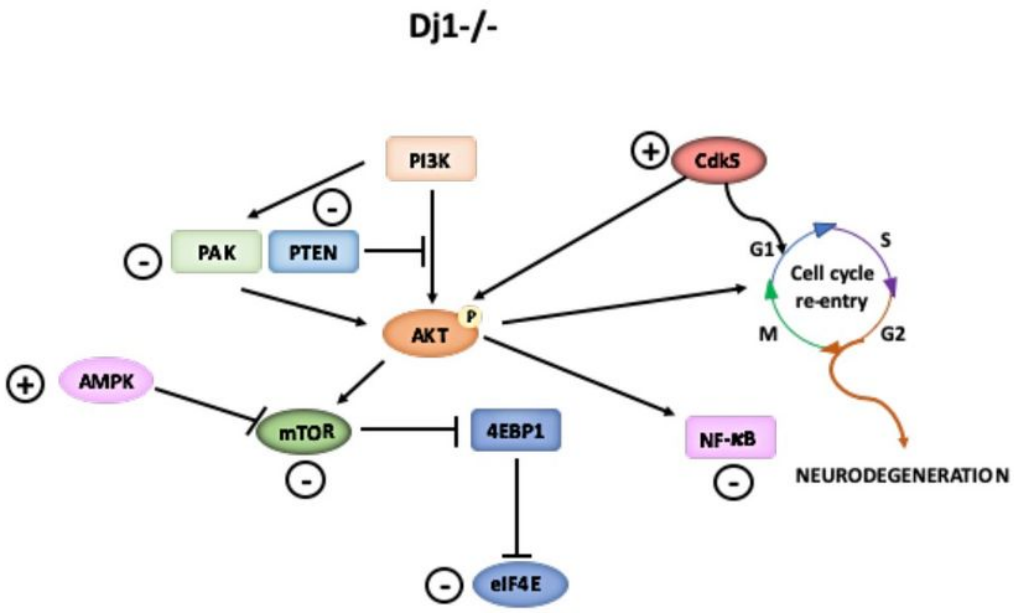

Figure 5

Schematic view of pathways induced and inhibited according to enrichment and biochemical analysis, that may lead to cell cycle re-entry and neurodegeneration in DJ-1 knockout neurons (see main text for further explanation).

Supplementary Files

This is a list of supplementary files associated with this preprint. Click to download.

- TableS1Totalproteinlist.xlsx
- SupplementaryFigure1.pdf
- TableS3PhosphoSTYSites.xlsx
- TableS2Significantproteinlist.xlsx

- SupplementaryFigure2.pdf